JOURNAL OF GUIDANCE, CONTROL, AND DYNAMICS
Vol. 28, No. 5, September–October 2005

Engineering Notes

ENGINEERING NOTES are short manuscripts describing new developments or important results of a preliminary nature. These Notes should not exceed 2500 words (where a figure or table counts as 200 words). Following informal review by the Editors, they may be published within a few months of the date of receipt. Style requirements are the same as for regular contributions (see inside back cover).

Cooperation Strategy of Unmanned Air Vehicles for Multitarget Interception

Rong Zhu*
Tsinghua University,
100084 Beijing, People's Republic of China
Dong Sun†
City University of Hong Kong,
Hong Kong, People's Republic of China
and
Zhaoying Zhou‡
Tsinghua University,
100084 Beijing, People's Republic of China

I. Introduction

IT is a trend that future unmanned air vehicles (UAVs) will be designed to make tactical decisions automatically and be cooperative in groups to achieve high-level complex missions. Consider a mission that a group of UAVs are required to intercept several known targets. A number of threats exist in the region of interest, some known a priori, others arise or become known only when UAVs maneuvers into their proximity. An optimal cooperation problem must be addressed to yield an optimum resource allocation among UAVs, to enhance the mission success and, furthermore, to optimize the fly trajectories for all UAVs in the action. This optimal cooperation problem can be decomposed into subproblems of path planning, resource-target management, trajectory generation, and UAVs' autonomous control.[1]

Path planners are generally divided into local and global,[2] in which dynamics of vehicles are usually not considered. The global planner works online and needs to be replanned when environment changes. The local planner works offline and may be trapped in a local minimum of the criterion function. To overcome these drawbacks, in this paper, we propose to incorporate a global path planning with a local trajectory generation.

The issue of UAVs' cooperation has been investigated by researchers. Beard et al.[1] and Chandler et al.[3] proposed a systematic architecture including target manager, path planner, intercept manager, and trajectory generator. A modified Voronoi diagram (see Ref. 4) and Eppstein's k-best paths algorithm[5] were used to generate paths for UAVs. The trajectory generation problem was solved via a nonlinear filter that accounts for the dynamic constraints of the vehicles.

The Voronoi diagram is a fundamental structure commonly used in path planning (see Refs. 6 and 7). The resulting Voronoi polygon edges, with threats into convex cell, constitute a set of lines that are equidistant from the closest threats and are thereby designed as path lines of vehicles. However, it is generally difficult to guide a UAV to fly exactly along a specific line. Comparatively, it would be easier and more reasonable for a UAV to track along a set of specific waypoints. In this Note, we use Delaunay triangulation instead of a Voronoi diagram to generate waypoint-based paths. Delaunay triangulation is a geometric structure defined as a straight-line dual of the Voronoi diagram (see Ref. 8), the edges of which connect two neighboring Voronio cells, that is, threats. Midpoints of Delaunay edges have the maximum distances to the closest threats and, thus, can be regarded as candidates of waypoints of vehicles. An incremental algorithm[9] can be used in our study to update the Delaunay triangulation when new pop-up threats emerge.

Traditionally, the trajectory planning is done either from a purely geometrical point of view based on geometric constraint, or by numerical optimization. The geometric solution only considers the problem of finding a geometrically feasible path amongst a set of given points in a cluttered environment,[10,11] but does not take dynamic models of vehicles into account. In contrast, the numerical optimization method considers dynamic models, dynamic constraints, and input bounds when generating a path, which optimizes performance criterions.[12] In this Note, we propose a novel waypoint-based numerical trajectory optimization based on criterions of shortpath and lowturning with consideration of dynamic models of UAVs, so that the method can be easily realized in applications.

II. Cooperation Architecture

Figure 1 shows the proposed cooperation architecture. It is assumed that each individual UAV flies at different preassigned altitudes from each other to avoid collision.

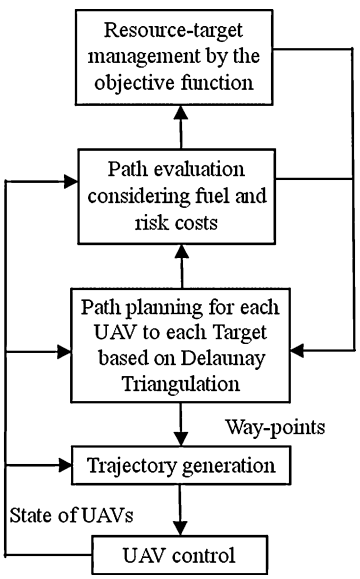

Fig. 1 System architecture for UAVs' cooperation.

Received 4 November 2004; revision received 13 April 2005; accepted for publication 21 April 2005.

*Associate Professor, Department of Precision Instruments and Mechanology; zrwzwyj@sh163.net.
†Associate Professor, Department of Manufacturing Engineering and Engineering Management; medsun@cityu.edu.hk.
‡Professor, Department of Precision Instruments and Mechanology.

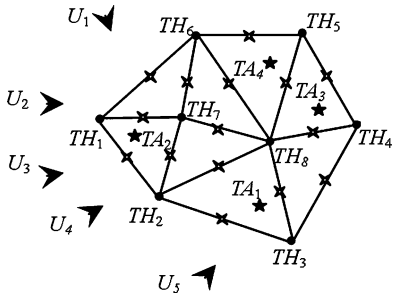

Fig. 2 Threat-based Delaunay triangulation: ➤ UAVs; ★, targets; ●, threats; and ×, midpoints of Delaunay edges.

III. Path Planning

The objective of the path planning is to generate an optimal waypoint-based path for an individual UAV to fly toward a specific target with the minimum fuel expenditure and risk from threats. In this Note, an approximation optimal algorithm based on geometric Delaunay triangulation is used for the path planning. The procedure mainly comprises the following three steps.

A. Construct a Delaunay Triangulation by Using Threats as Vertices

Consider UAVs $\{U_i\} = \{U_1, U_2, \ldots, U_N\}$, targets $\{TA_j\} = \{TA_1, TA_2, \ldots, TA_M\}$, and threats $\{TH_k\} = \{TH_1, TH_2, \ldots, TH_O\}$, where N, M, and O represent the numbers of the UAVs in service, the targets, and the existing known threats at the decision time, respectively. A Delaunay triangulation structure is constructed to partition the whole routing region into several triangles as shown in Fig. 2, where the threats are used as vertices. Midpoints of the resulting Delaunay edges are equidistant from the two neighboring threats, that is, the two endpoints of the Delaunay edges, and thereby their distances to the neighboring threats are maximized. These midpoints of Delaunay edges are selected as candidates of waypoints of UAVs. To avoid large hazards, the midpoints whose distances to the neighboring threats are smaller than the predefined threshold will not be considered.

B. Generate a Weighted Tree with Midpoints of Delaunay Edges as Nodes of Tree

A weighted tree is then generated by using the eligible midpoints of Delaunay edges, denoted by $P = \{p_1, \ldots, p_n\}$. These midpoints are treated as nodes of the tree. Connecting any pair of midpoints within same triangles forms tree edges. Weights of tree edges are evaluated by synthesizing two costs: the threat cost that indicates the risk level and the length cost that indicates the fuel expenditure. Figure 3 shows an example of generating a path from U_i to TA_j.

Assume that the threat cost for traveling across a waypoint is based on a UAV's exposure to radars located at threat points, and that the radar signature is uniform in all directions and is proportional to the distance (from the waypoint to the threat) to the fourth power.[13] Thus, the threat cost associated with the midpoint P_i is given by

$$J_{\text{threat}}^{P_i} = \sum_{j=1}^{O} \frac{1}{d_{P_i,j}^4} \tag{1}$$

where $d_{P_i,j}$ is the distance from P_i to the jth threat. $J_{\text{threat}}^{P_i}$ is further normalized in the range [0,1] as $\mu_{\text{threat}}^{P_i}$.

Some no-fly zones can be identified via evaluating threat costs of triangle regions. Select a key point for each triangle region, for example, the center of the triangle. Calculate the threat cost of the key point using Eq. (1), and then judge if the calculated threat cost is larger than a predefined threshold. If it is, this triangle region is regarded as no-fly zone and will be removed from the flying region when searching for the optimal path.

The length cost of the tree edge is simply represented by the length of the edge and is normalized in the range [0,1] as μ_{length}^{k}.

The sum of the normalized threat and length costs yields the weight of the tree edge expressed by

$$W_k = \alpha \cdot \left(\mu_{\text{threat}}^{h_k} + \mu_{\text{threat}}^{t_k}\right)/2 + \beta \cdot \mu_{\text{length}}^{k} \tag{2}$$

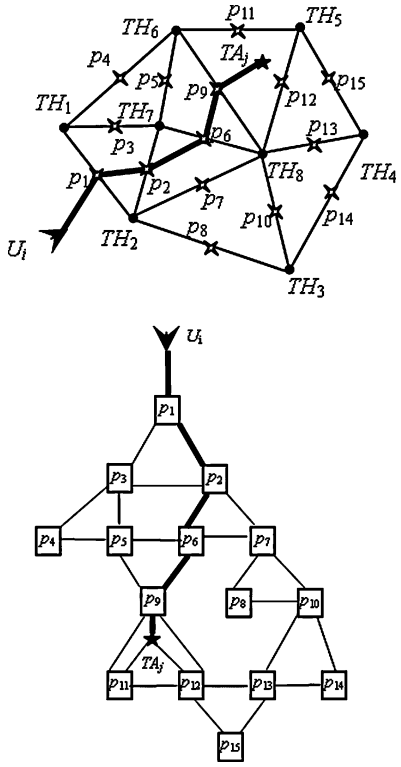

Fig. 3 Weighted tree formed by midpoints of Delaunay edges.

where W_k is the weight of the kth edge of the tree, α and β are gains for placing weight on risk and fuel perspectives depending on the particular mission scenario; and $\mu_{\text{threat}}^{h_k}$ and $\mu_{\text{threat}}^{t_k}$ are the normalized threat costs of two endpoints of the kth edge. The normalized threat costs of the start and target points of the UAV, for example, U_i and TA_j in Fig. 3, are assumed to be zero.

C. Search for an Optimal Path from Start to Target in Weighted Tree

This procedure is to find out an optimal path connecting U_i and TA_j in the weighted tree, with the property that the sum of weights of all connecting edges is minimized over all possible paths, that is,

$$\sum W_k \rightarrow \text{minimum}$$

All nodes lying on the optimal path are waypoints of the path. As seen in Fig. 3, the optimal path connecting U_i and TA_j is shown by bold lines, where p_1, p_2, p_6, and p_9, together with the start point U_i and the target point TA_j, are waypoints of the path.

IV. Cooperation Design of Resource-Target Management

The resource-target management is to assign one specified target for each individual UAV based on objectives of minimizing fuel expenditures and risks and maximizing the team power, for example, the force, that is, the number of UAVs prosecuting the same target, and the spread of intercepted targets, that is the number of targets to be intercepted. Create a cost-based objective function $f(\{U_i\}, \{TA_j\}, \{TH_k\})$ that incorporates all desired objectives,

$$f(\{U_i\}, \{TA_j\}, \{TH_k\}) = \sum_{i=1}^{N} (\alpha \cdot \mu_{\text{threat},i,j_i} + \beta \cdot \mu_{\text{length},i,j_i}) + \mu_{\text{force}}[j_1, \ldots, j_N] + \mu_{\text{spread}}[j_1, \ldots, j_N] \tag{3}$$

where $[j_1, \ldots, j_N]$ denotes a resource-target assignment, which indicates that targets $TA_{j_1}, \ldots, TA_{j_N}$ are assigned to UAVs denoted by $U_1, \ldots, U_N$, respectively; $\mu_{\text{threat},i,j_i}$ and $\mu_{\text{length},i,j_i}$, both in the range [0,1], are the normalized threat and length costs of the path for U_i to TA_{j_i}, which are defined as the sum of the threat costs of all waypoints lying on the path and the sum of edge lengths

of the path; $\mu_{\text{force}}(j_1, \ldots, j_N)$ and $\mu_{\text{spread}}(j_1, \ldots, j_N)$ represent the force and spread costs of the team associated with the assignment $[j_1, \ldots, j_N]$, expressed by sigmoid functions[1] as

$$\mu_{\text{force}} = \sum_{\{TA_j\}} \left[2 - \frac{2}{1 + e^{-2\cdot[m(j)-1]}} \right]$$

$$\mu_{\text{spread}}[n(TA)] = 2 - \frac{2}{1 + e^{-2\cdot[n(TA)-1]}}$$

respectively, in which $m(j)$ is the number of the UAVs assigned to prosecute TA_j and $n(TA)$ is the number of targets intercepted by UAVs.

The optimal solution is to minimize the objective function $f(\{U_i\}, \{TA_j\}, \{TH_k\})$ to obtain an optimal assignment $[j_1, \ldots, j_N]$. A model of the optimal cooperation is expressed as

$$\min_{\{U_i\},\{TA_j\}} f(\{U_i\}, \{TA_j\}, \{TH_k\}) \tag{4}$$

As the calculation increases as the team scale increases, the complexity of finding an optimal solution relies on the scale of the resource and target. For a team of UAVs with the number of M to intercept N targets, it is needed to check N^M possible assignments, which implies that the computation time for solving the optimal team assignment is in the order of N^M.

The resource-target management just described needs to be updated when pop-up situations happen.

V. Trajectory Generation

In this section, a numerical trajectory optimization is proposed based on criterions of shortpath and lowturning. The shortpath aims to minimize the trajectory length to minimize the fuel expenditure of the UAV. The lowturning aims to minimize the turning rate and the variation of the turning rate so as to ensure a stable and valid flight of UAVs.

We now consider the trajectory design of the UAV U_i to pass through specific waypoints, that is U_i, p_1, p_2, p_6, p_9, and TA_j, to reach the target TA_j, as shown in Fig. 4. To reduce the risk to the greatest extent, the fly trajectory is designed to intersect orthogonally the corresponding Delaunay edges at the waypoints p_1, p_2, p_6, and p_9. The heading direction when the UAV flies across these waypoints is shown by the arrows in Fig. 4. The whole trajectory from U_i to TA_j can be divided into a set of consecutive segments that connect two neighboring waypoints, for example, U_i to p_1, p_1 to p_2, etc. These trajectory segments can be classified as two typical cases: transition between two points, A and B, for example, p_9 to TA_j and transition between two path segments, for example, p_1 to p_2. In the former situation, as seen in Fig. 5a, there is no heading constraint at B, whereas in the latter situation, as seen in Fig. 5b, there is heading constraint at B.

A dynamic model of UAVs[1,14] for the constant altitude maneuvers, formulated as follows, is employed to generate trajectories for

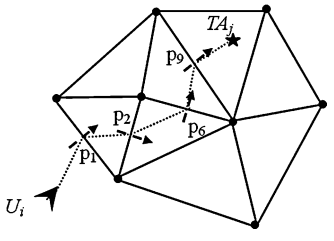

Fig. 4 Waypoints of the path for U_i to TA_j.

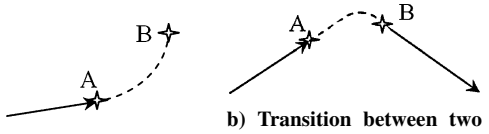

a) Transition from point A to point B

b) Transition between two path segments from point A to point B

Fig. 5 Two typical trajectory problems.

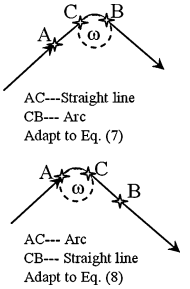

Fig. 6 Trajectory path consisting of a straight line and an arc.

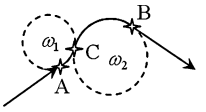

Fig. 7 Trajectory composed of two segments of two circles.

these two cases:

$$\dot{X} = V \cdot \cos\psi, \qquad \dot{Y} = V \cdot \sin\psi, \qquad \dot{\psi} = \omega, \qquad \dot{h} = 0 \tag{5}$$

where (X, Y) is the desired inertial position of the UAV and ψ, V, h, and ω are the desired heading angle, speed, altitude, and turning rate constrained by the dynamic capability of the UAV, respectively.

For transition between two points without heading constraint at B, the trajectory is designed to be a circular arc based on lowturning objective, namely, the turning rate of the UAV is designed as small as possible. The turning rate ω is then calculated from Eq. (5):

$$\omega = \frac{2 \cdot V \cdot (\Delta X_{A-B} \cdot \sin\psi_A - \Delta Y_{A-B} \cdot \cos\psi_A)}{\Delta X_{A-B}^2 + \Delta Y_{A-B}^2} \tag{6}$$

where ΔX_{A-B} and ΔY_{A-B} denote distances between A and B along X (north) and Y (east) axes and ψ_A denotes the real heading angle of the UAV at A.

For the trajectory between two path segments, we propose that an optimal trajectory between two path segments comprises a straight line and a transitional circular arc with the maximum turn radius based on shortpath and lowturning criterions, which is justified in the Appendix.

Figure 6 shows a generated trajectory. The turning rate ω along the arc is calculated from Eq. (5), if

$$\frac{\Delta X_{A-B} \cdot (\cos\psi_B - \cos\psi_A) + \Delta Y_{A-B} \cdot (\sin\psi_B - \sin\psi_A)}{\cos(\psi_A - \psi_B) - 1} \geq 0$$

$$\omega = \frac{V \cdot [\cos(\psi_A - \psi_B) - 1]}{\Delta X_{A-B} \cdot \sin\psi_A - \Delta Y_{A-B} \cdot \cos\psi_A} \tag{7}$$

if

$$\frac{\Delta X_{A-B} \cdot (\cos\psi_B - \cos\psi_A) + \Delta Y_{A-B} \cdot (\sin\psi_B - \sin\psi_A)}{\cos(\psi_A - \psi_B) - 1} < 0$$

$$\omega = \frac{V \cdot [1 - \cos(\psi_A - \psi_B)]}{\Delta X_{A-B} \cdot \sin\psi_B - \Delta Y_{A-B} \cdot \cos\psi_B} \tag{8}$$

where ψ_B is the desired heading angle at B.

Note that the turning rate ω must meet the dynamic constraint of the vehicle, for example, $-|V|/r_{\min} \leq \omega \leq |V|/r_{\min}$, where $r_{\min}$ is the minimal turn radius of the UAV. If such constraint is not satisfied, ω is set as $\omega_0 = \text{sign}(\omega) \cdot |V|/r_{\min}$ and the straight line in the trajectory is replaced by another tangent circular arc, as shown in Fig. 7. The turning rates of the two circular arcs, ω_1 and ω_2, satisfy the following relationship from Eq. (5):

$$\Delta X_{A-B} = (V/\omega_1) \cdot (\sin\psi_C - \sin\psi_A) + (V/\omega_2) \cdot (\sin\psi_B - \sin\psi_C)$$

$$\Delta Y_{A-B} = -(V/\omega_1) \cdot (\cos\psi_C - \cos\psi_A) - (V/\omega_2) \cdot (\cos\psi_B - \cos\psi_C) \tag{9}$$

where ψ_C is the desired heading angle at the joint point C between the two tangent arcs. By use of Eq. (9), ω_1 and ω_2 can be solved because one of them was set as ω_0 earlier.

The preceding two-waypoint trajectory can be further extended to multiwaypoint trajectory cases by connecting consecutive two-waypoint segments.

VI. Mission Scenario

Consider a mission in which a six-UAV team intercepts four known targets. The targets are located in a region where several threats are distributed. The task is to visit and intercept these targets while minimizing the risk of losing UAVs and maximizing the task efficiency. Figure 8 shows the mission scenario, where triangles represent UAVs denoted by U1–U6, pentagrams represent targets denoted by TA1–TA4, and dots represent threats.

Assume $\alpha, \beta = 0.5$. Figure 9 shows the objective functions for various resource-target assignments of this team that combine fuel expenditures, risks, force, and spread objectives. The numbers in parenthesis indicate the numbers of UAVs assigned to different targets. For example, (2,4) indicates that two UAVs are allocated to one target and the other four are allocated to another target. In Fig. 9 we only labeled the optimal resource-target assignment with minimum cost for each vehicle assignment, where numbers in square brackets indicate the sequence numbers of targets intercepted by $U_1 - U_6$, respectively. For instance, [2 3 3 2 1 1] is the optimal resource-target assignment for the vehicle assignment (2,2,2), which indicates that

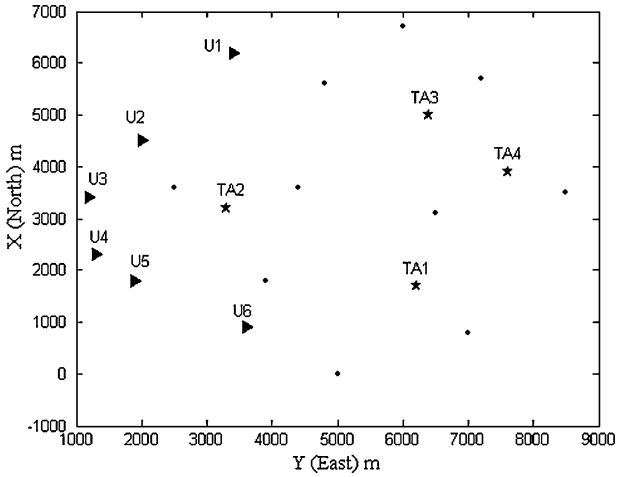

Fig. 8 Mission scenario.

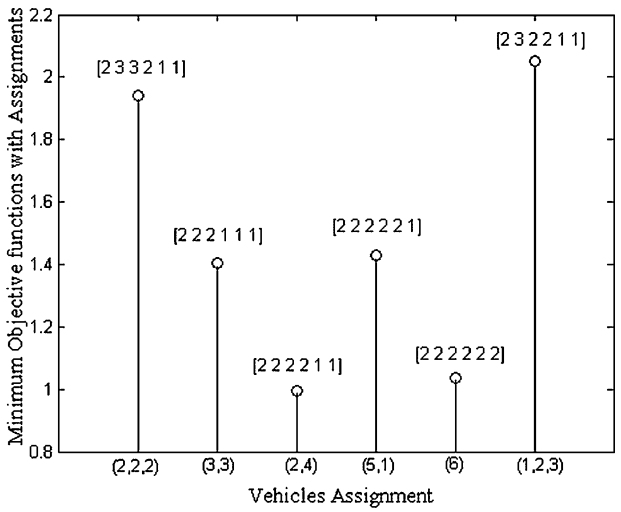

Fig. 9 Objective functions and corresponding resource-target assignments.

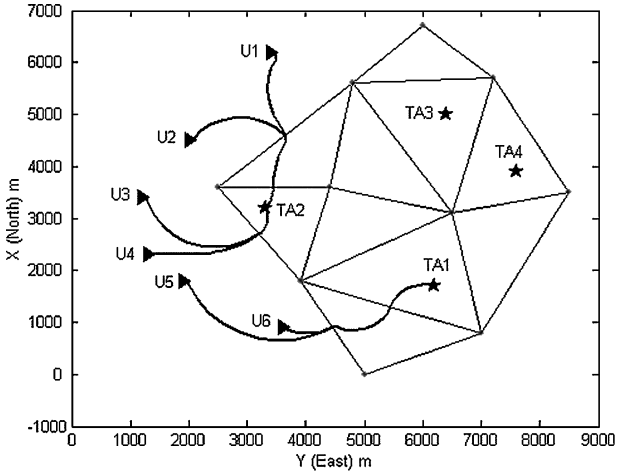

Fig. 10 Mission scenario: U1–U4 intercept TA2, U5 and U6 intercept TA1.

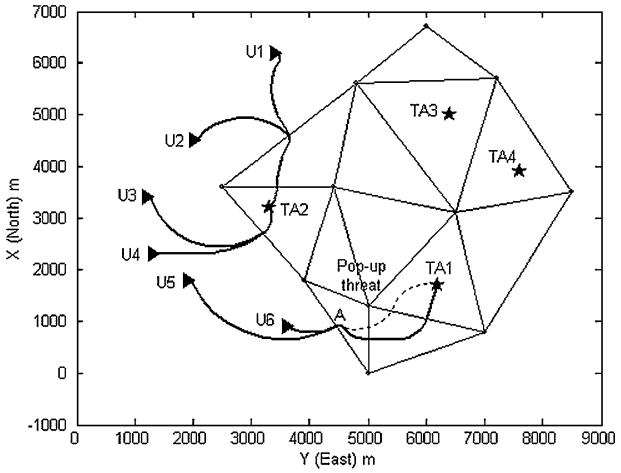

Fig. 11 Updated trajectories after a pop-up threat is detected.

U1 and U4 intercept TA2, U2 and U3 intercept TA3, and U5 and U6 intercept TA1. When an overall view of the objective functions in Fig. 9 is given it is noted that the resource-target assignment [2 2 2 2 1 1] is optimal because its value of the objective function is minimum. Specifically, the optimal assignment is that U1–U4 intercept TA2, and U5–U6 intercept TA1.

Assume that the minimal turn radius of the UAVs in the team is 100 m. Figure 10 shows trajectory paths of the UAVs associated with the optimal assignment [2 2 2 2 1 1], where the threat-based Delaunay triangulation is shown as well. Note that all UAVs have different and preassigned altitudes for avoiding collision.

The pop-up scenario is shown in Fig. 11. A pop-up threat is detected at the time when U5 and U6 arrive at A. The Delaunay triangulation around the new threat is then recomposed, and the subsequent trajectories are redesigned to escape the new threat. Here the solid and dotted lines denote the updated and initial trajectories, respectively.

After TA1 and TA2 are intercepted successfully, the UAVs that are still in service will be reassigned to prosecute the remaining targets TA3 and TA4 according to the current situation of the UAVs and the battlefield. This process is ignored in this simulation.

VII. Conclusions

This paper presents an optimal approach to deal with cooperation problems for a group of UAVs to intercept multiple targets. A waypoint-based path planning is proposed by creating a Delaunay weighted tree and searching for an optimal path in the tree with the minimum fuel expenditure and risk level. A cost-based objective

function is designed for optimizing the resource-target assignment, which combines threat and length costs of paths, as well as force and spread costs of the team. A fly trajectory that consists of one or two arcs and/or a straight line is generated taking into consideration UAV dynamics, which can be extended to multiwaypoint trajectory cases. A simulation of a cooperation mission by a six-UAV team is performed to validate the effectiveness of the proposed approach.

Appendix: Optimal Trajectory Between Two Path Segments

A trajectory between two path segments typically comprises of two straight lines, for example, AF and EB in Fig. A1, where the points F and E are tangential points, respectively, and a transitional arc of a tangent circle connecting the two lines,[1,15] shown as the solid line in Fig. A1. The length L_{AB} of the trajectory from A to B can be calculated by

$$L_{AB} = L_{AD} + L_{DB} + (L_{FE} - L_{FD} - L_{DE})$$

$$L_{FE} = R_1 \cdot \Delta\psi, \qquad L_{FD} = L_{DE} = R_1 \cdot tg(\Delta\psi/2) \qquad \text{(A1)}$$

where L_{AD}, L_{DB}, L_{FD}, and L_{DE} are lengths of straight lines AD, DB, FD, and DE, respectively; D is the intersection point of the two path segments; L_{FE} is the length of the transitional arc between F and E; R_1 denotes the radius of the tangential circle; $\Delta\psi(\leq \pi)$ denotes the joint angle between two path segments.

When it is considered that $L_{FE} - L_{FD} - L_{DE} = 2 \cdot R_1 \cdot [(\Delta\psi/2 - tg(\Delta\psi/2)] \leq 0$ and that L_{AD} and L_{DB} are fixed, L_{AB} can be minimized by maximizing the absolute value of $L_{FE} - L_{FD} - L_{DE}$ according to Eq. (A1), which can be done through maximizing the radius of the circle R_1. The tangent circle with the maximal radius R_2 is shown with dashed line in Fig. A1. As a result, based on shortpath and lowturning, the trajectory between two path segments from A to B consists of a straight line (AG) and a transitional circular arc (GB) with the maximum turn radius.

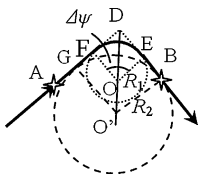

Fig. A1 Trajectory between two path segments.

References

[1]Beard, R. W., Mclain, T. W., Goodrich, M. A., and Anderson, E. P., "Coordinated Target Assignment and Intercept for Unmanned Air Vehicles," *IEEE Transaction on Robotics and Automation*, Vol. 18, No. 6, 2002, pp. 911–922.

[2]Sasiadek, J. Z., and Duleba, I., "3D Local Trajectory Planner for UAV," *Journal of Intelligent and Robotic Systems*, Vol. 29, No. 2, 2000, pp. 191–210.

[3]Chandler, P. R., Pachter, M., and Rasmussen, S., "UAV Cooperative Control," *Proceedings of the American Control Conference*, Inst. of Electrical and Electronics Engineers, New York, 2001, pp. 50–55.

[4]Sedgewick, R., *Algorithm*, 2nd ed., Addison–Wesley, Reading, MA, 1998, pp. 124–140.

[5]Eppstein, D., "Finding the *k* Shortest Paths," *SIAM Journal on Computing*, Vol. 28, No. 2, 1999, pp. 652–673.

[6]Takahashi, O., and Schilling, R. J., "Motion Planning in a Plane Using Generalized Voronoi Diagrams," *IEEE Transactions on Robotics and Automation*, Vol. 5, No. 2, 1989, pp. 143–150.

[7]Hoff, K. I., Culver, T., Keyser, J., Lin, M. C., and Manocha, D., "Interactive Motion Planning Using Hardware-Accelerated Computation of Generalized Voronoi Diagrams," *Proceedings of the 2000 IEEE International Conference on Robotics and Automation*, Vol. 3, Inst. of Electrical and Electronics Engineers, Piscataway, NJ, 2000, pp. 2931–2937.

[8]Berg, M. D., Kreveld, M. V., Overmars, M., and Schwarzkopf, O., *Computational Geometry: Algorithms and Applications*, 2nd ed., Springer-Verlag, Berlin, 2000, pp. 185–207.

[9]Guibas, L. J., Knuth, D. E., and Sharir, M., "Randomized Incremental Construction of Delaunay and Voronoi Diagrams," *Algorithmica*, Vol. 7, No. 4, 1992, pp. 381–413.

[10]Wang, Y., and Lane, D., "Subsea Vehicle Path Planning Using Nonlinear Programming and Constructive Solid Geometry," *IEE Proceedings of Control Theory and Applications*, Vol. 144, Inst. of Electrical Engineers, Stevenage, England, U.K., 1997, pp. 143–152.

[11]Jackson, J., and Crouch, P., "Curved Path Approaches and Dynamic Interpolation," *IEEE Aerospace and Electronic Systems Magazine*, Vol. 6, No. 2, 1991, pp. 8–13.

[12]Betts, J., "Survey of Numerical Methods for Trajectory Optimization," *Journal of Guidance, Control, and Dynamics*, Vol. 21, No. 2, 1998, pp. 193–207.

[13]Huang, J., Wu, Z., and Xiang, J., "Assessment of Aircraft Combat Survivability Enhanced by Combined Radar Stealth and Onboard Electronic Attack," *Transactions of Nanjing University of Aeronautics and Astronautics*, Vol. 17, No. 2, 2000, pp. 150–156.

[14]Anderson, E. P., and Beard, R. W., "An Algorithmic Implementation of Constrained Extremal Control for UAVs," *AIAA Guidance and Control Conference*, AIAA, Reston, VA, 2002, pp. 2002–4470.

[15]Boissonnat, J. D., Cerezo, A., and Leblond, J., "Shortest Paths of Bounded Curvature in the Plane," *Proceedings of the 1992 IEEE International Conference on Robotics and Automation*, Vol. 3, Inst. of Electrical and Electronics Engineers Computer Society Press, Los Alamitos, CA, 1992, pp. 2315–2320.